

## Phase-Parameter Representation of Neutron-Proton Scattering from 13.7 to 350 Mev\*

M. H. HULL, JR., K. E. LASSILA, H. M. RUPPEL, F. A. McDONALD, AND G. BREIT  
*Yale University, New Haven, Connecticut*

(Received January 30, 1961)

Results of gradient searches, by means of an IBM 704 machine, for phase parameters representing neutron-proton scattering are reported. The analysis made use of most available measurements. The number of "measurements" used in the final searches was 293 with 35 additional ones which were used to obtain composite values. Most of the fits join reasonably smoothly to the  $^3S_1$  phase shift curve at low energies. The validity of charge independence was assumed and the more probable among the  $T=1$  phase-parameter sets obtained in a previously described series of searches for phase-parameter fits to  $p$ - $p$  data were therefore employed for this  $T$ . The one-pion exchange values were used for the larger  $L$  and  $J$ . Independent sets of searches started with phase parameters corresponding to the Gammel-Christian-Thaler potential, and the

Gammel-Thaler potential, respectively. The procedure was varied by employing a weighted mean of fits obtained from the two different starting points as a new starting set and other devices described in the text. The final fits are appreciably better than the starts, the mean square deviation being reduced by a factor  $\sim 20$  in some cases. A rough division of the final fits into related families according to the behavior of the parameters  $K_3$  and  $\rho_3$  can be made. The value of additional measurements and especially those of the triple-scattering parameters and polarization correlation is pointed out. Tests on reasonableness of one of the better fits from the point of view of representation by a static potential have been made, with satisfactory results.

### I. INTRODUCTION

THE analysis of nucleon-nucleon scattering data in terms of energy-dependent shifts and coupling parameters, referred to collectively as phase parameters below, has been described for the proton-proton case by Breit, Hull, Lassila, and Pyatt.<sup>1</sup> The application of the same gradient search method to neutron-proton scattering data is described in the present paper. Some preliminary results of this work have been previously reported<sup>1</sup> but the treatment of data, many of the more recent modifications of the fits, and the systematic presentation of evidence for and against the various fits have not been previously presented. In the neutron-proton case the measurements are not so plentiful and only in the vicinity of 90 Mev incident neutron energy has it been possible or convenient to lump measurements to any extent. The number of measurements used in searches finally was 293, with 35 additional ones having been used to obtain lumped values. About half of the polarization data became available only for the most recent adjustments of phase parameters.

The comparative paucity of observations in the  $n$ - $p$  case, and lack of triple-scattering data except for a few values at 310 Mev, leads one to expect that more than one set of phase parameters can be found to give a fit. This is indeed the case and the present analysis is not claimed to have found all possible fits. In the  $p$ - $p$  work the triple-scattering data were not plentiful enough to dominate the searches when the gradient was calculated with measurements in a wide energy range. They served nevertheless to select from among several otherwise satisfactory fits and if they were

available they would probably be helpful in the present instance as well. The calculations reported here do not provide a unique fit, therefore, to the  $n$ - $p$  scattering data, but they do supply sets of phase parameters which represent the data more faithfully than any other sets known to the authors. Relatively more reliance had to be placed on theoretical criteria such as the reasonable variation of the logarithmic derivatives of the wave functions with energy than in the proton-proton case.

### II. DATA USED AND STARTING POINTS

Most of the data available for this analysis are contained in the collection by Hess<sup>2</sup> and, with some exceptions which are mentioned below, all of the  $n$ - $p$  data collected by Hess have been used as seen in Table I which lists the data taken from that reference and provides comments on their use. Data of Hess' reference C7 at 90 Mev were omitted in favor of other measurements available at this energy because the omitted ones were given for  $10^\circ$  angular spreads and the procedure used was not directly adaptable to such data input. These data, if plotted at their mean angle, compare well with the lumped values used in the searches although a few measurements at the higher angles appear a little low, and the omitted data are, therefore, well fitted by the theoretical curves. The 93-Mev data of Hess' reference S6 consisting of six points in the angular range from  $155.4^\circ$  to  $177.5^\circ$  were not included in the 90-Mev lumped measurements, but agree well with them. Similarly the 4 measurements of Hess' reference G4 listed for "95-100" Mev were not used.

The more recent data employed in the search and not contained in the collection by Hess are listed in Table II. Except for the polarization measurements at 156 Mev, these were not available until the most recent calculations were carried out. When compared with predictions of case YLAN3 (cf. Table III), it was found

\* This research was supported by the U. S. Atomic Energy Commission and by the Office of Ordnance Research, U. S. Army.

<sup>1</sup> G. Breit, M. H. Hull, K. Lassila, and K. D. Pyatt, Phys. Rev. **120**, 2227 (1960) referred to hereafter as "I." A report on an earlier stage of the results for both  $n$ - $p$  and  $p$ - $p$  scattering analysis has been given by G. Breit at the London Conference on Nuclear Forces and the Few Nucleon Problem, July 1959. The report will appear in the proceedings of that conference, to be published.

<sup>2</sup> W. N. Hess, Revs. Modern Phys. **30**, 368 (1958).

TABLE I. Treatment of data given in W. N. Hess [Revs. Modern Phys. 30, 368 (1958)]; where Hess gives renormalized values of  $\sigma(\theta)$ , these are used.

Quantity	Energy incident (Mev)	Angular range (degrees), c.m. system	Number of angles	Remarks
$\sigma$	13.7	36.1- 86.3	8	The datum point $\sigma(15.7^\circ) = 33.6 \pm 8.8$ mb is not used because the experimenters (reference R1 of Hess) seriously question this point
$\sigma$	14.1	48 -173	14	In earlier searches, these data were run at common energy 27.8 Mev.
$\sigma$	27.2 <sup>a</sup>	76 -179	6	
$\sigma$	28.4 <sup>a</sup>	11.3- 94.2	10	
$\sigma$	42.0	62 -180	13	
$\sigma$	90, 91	5.1-180	33	
				All data of references H3, C6, F2, W2, and S7 of Hess are used, and values at same angle or angle differing by $<3^\circ$ are averaged. Run at 90 Mev.
$P$	95	22.5-159.5	15	Hess lists energy as 140-145 Mev; 143 Mev was used for simplicity, as $P$ data exist at this energy. See Table II.
$\sigma$	105	6.2- 61.4	7	
$\sigma$	130	25 -155	14	
$\sigma$	137	6.3- 61.8	7	
$\sigma$	143	19.3- 58.3	5	
$\sigma$	156	50 -180	19	
$\sigma$	172	77.5-180	9	
$\sigma$	215	76.9-180	8	
$\sigma$	260	37.7-180	15	
$\sigma$	290, 300	10.7-180	20	
$P$	310	21.6-164.9	17	All data run at 300 Mev.
$P$	350 <sup>b</sup>	46.3-158.2	12	

<sup>a</sup> The cross-section data at 27.2 Mev, from reference B3 of Hess, were normalized, according to the authors, to a total cross-section value of 360 mb read from a graph given by R. K. Adair, Revs. Modern Phys. 22, 249 (1950). The data at 28.4 Mev were normalized by Hess to a total cross section of 342 mb read from Hess' Fig. 1. The persistence through searches YLAN0, YLAN1, YLAN2, and YLAN2M of a systematic difference between these experimental measurements and theoretical values calculated from phase parameters having a smooth energy dependence and giving fits to data at adjacent energies suggested a reexamination of the normalization. The total  $n-p$  cross section data listed by Hess, which contained some recent data that were not available to Adair, were plotted in the energy range 10-150 Mev. Values of total  $n-p$  cross section at 27.2 and 28.4 Mev were read as 337 and 320 mb, respectively. The published angular distribution data were fitted by least squares by  $a + b \cos\theta + c \cos^2\theta$  and this function was integrated over all solid angles to give the total cross section, which was made to agree with 337 and 320 mb, respectively. This resulted in a reduction of 8% at 28.4 Mev and 5.5% at 27.2 Mev in the values given by Hess. These renormalized data are plotted in the figures to be described below, and were used in the searches YLAN3 and YLAN3M. It may be noted that the renormalization has little effect on final results, since the uncertainties are large and the resulting statistical weights are therefore small. Data taken directly from the Hess collection raise values of the mean-square error  $D$  in the last two lines of Table III by about 0.2. The authors wish to thank Professor Adair for a conversation in connection with the present normalization.

<sup>b</sup> These data were used only in the most recent search, YLAN3M. Extrapolation of the phase-parameter curves to 350 Mev gave values which led to theoretical representations in good agreement with the data. Subsequent searches produced only modest improvements in the fit.

that these data were very well fitted without searching; an exception being the low-angle measurements at 77 Mev, which were higher than predicted. The high-angle measurements at 77 Mev were fitted nearly perfectly.

The initial values of the phase parameters  $\theta^{S_1}, \rho_1, K_1, \theta^{D_1}, \delta^{D_2}, \theta^{D_3}, \rho_3, K_3, \theta^{G_3}, \delta^{G_4}$ , in the notation of I, Eqs. (6)-(6.4), were obtained from phenomenological potentials, as described in text accompanying Table III, and  $\theta^{G_5}, \rho_5$  were started at values calculated in first Born approximation from the one-pion exchange potential

(OPEP). All 12 phase parameters listed were allowed to vary in the searches, except in cases YLAN3 and YLAN3M, as noted in the description of these searches following Table III.

The validity of charge independence was assumed and the phase-parameters for isotopic triplet states with smaller angular momentum were therefore taken from fits YLAM(1) and YLAM(2) as the best available representations of  $p-p$  data described in I. Since they were started with phase parameters corresponding to

TABLE II. Quantities and energies in addition to those from the collection by Hess.

Quantity	Energy incident (Mev)	Angular range (degrees), c.m. system	Source	Number of angles	Remarks
$P$	77.0	20.6-159.2	a	17	Both sets of asymmetry data used and averaged together. 30.3 degree point dropped and 40.3 degree point error bar increased by factor 1.5 on advice from Dr. Warner and Dr. Tinlot.
$\sigma$	128.0	78.1-169.7	b	10	
$P$	128.0	78.1-169.7	b	10	
$P$	143.0	41.0-118.0	b	8	
$P$	156.0	68.0-154.0	c	5	
$P$	210.0	40.3-141.8	d	11	

<sup>a</sup> C. Whitehead, S. Tornabene, and G. H. Stafford, Proc. Phys. Soc. (London) 75, 345 (1960).

<sup>b</sup> R. Wilson (private communication).

<sup>c</sup> A. Roberts, J. H. Tinlot, and E. M. Hafner, Phys. Rev. 95, 1099 (1954).

<sup>d</sup> R. Warner and J. Tinlot (private communication). The authors wish to thank Dr. Warner and Professor Tinlot for communicating their results.

the Gammel-Thaler<sup>3</sup> phenomenological potential, it was formally consistent to use as starting values the phase parameters corresponding to the isotopic singlet potentials of Gammel, Christian, and Thaler<sup>4</sup> and of Gammel and Thaler<sup>5</sup> for the T=0 states. The phase parameters in T=1 states were not allowed to vary until the final stages of a search, when parallel shift gradients, of the type described in I, were carried out.

For states of larger angular momentum, phase parameters calculated in first order from the OPEP were used.<sup>6</sup> As in the  $p$ - $p$  searches described in I, the OPEP phase parameters were omitted if their value was less than 0.0005 rad. From 13.7 to 28.4 Mev, the maximum  $J$  value of phase parameters included in the OPEP calculation was 4 or 5; from 42 to 105 Mev it was 7 to 10; from 128 to 156 Mev it was 11; from 172 to 310 Mev it was 13. For several searches values of OPEP phase parameters corresponding to the  $\pi^+$  mass and the nonrelativistic approximation were used in both T=0 and T=1 states. For the most recent searches, the relativistic treatment<sup>6</sup> was employed and both the  $\pi^0$  and  $\pi^+$  masses entered the OPEP calculations, as described in I, Eqs. (5)-(5.3), even though the experimental uncertainties may not perhaps justify such refinements. Phase parameters in T=1 states which were initially of the OPEP type in YLAM but were searched in later stages at higher energies, were introduced into the corresponding  $n$ - $p$  search, YLAN3, by adding the searched *differences* obtained in the  $p$ - $p$  case to the  $n$ - $p$  T=1 OPEP values. With no intention of belaboring the point, one may remark that the addition of the differences occurred after several gradients of the YLAN3 search had been made, and that a small improvement in the fit to  $n$ - $p$  data was produced by the addition, indicating perhaps some consistency of results for high  $L$  and  $J$ . The  $n$ - $p$  searches and corresponding weighted mean-square error,  $D$  [cf. Eq. (2.3) of I], are summarized in Table III with a brief description of each search contained in the adjoining text. The parametrization of the scattering matrix given in Eqs. (6)-(6.4) of I was used throughout.

TABLE III. Values of  $D$  for  $n$ - $p$  gradient searches.

Search designation	Initial $D$	Final $D$
YLAN0	54.6	2.46
YLAN1	(54.6) 12.76	2.34
YLAN2	48.5	2.23
YLAN2M	2.19	1.96
YLAN3	13.02	1.64
YLAN3M	3.03	1.65

For search YLAN0 phase parameters in T=1 states

<sup>3</sup> J. Gammel and R. M. Thaler, Phys. Rev. **107**, 291 (1957).

<sup>4</sup> J. L. Gammel, R. S. Christian, and R. M. Thaler, Phys. Rev. **105**, 311 (1957). Hereafter referred to as "GCT."

<sup>5</sup> J. Gammel and R. M. Thaler, Phys. Rev. **107**, 1337 (1957). Hereafter referred to as "GT."

<sup>6</sup> G. Breit and M. H. Hull, Jr., Nuclear Phys. **15**, 216 (1960).

were used from YLAM(1); in T=0 states they were read from graphs of tabulated values given by Gammel, Christian, and Thaler.<sup>4</sup> The OPEP phase parameters were used for states with  $L > 5$  and for  $\theta_5^G$  and  $\rho_5$ . They were computed in first Born approximation without regard to mass difference for pions of different charge. In the gradient searches,  $\theta_5^G$  and  $\rho_5$  were allowed to vary with the phase parameters for smaller  $L$ . As noted in footnotes to Tables I and II, not all data finally used were available for the YLAN0 searches. A calculation of the mean-square error for all data, including the modified data at 27.8 and 28.1 Mev according to footnote a of Table I, gave 2.73 for YLAN0. The polarization at 77 Mev made most of the difference.

For search YLAN1 the phase shift  $K_3$ , which had been searched from initial negative to final positive values was replaced in YLAN0 by its starting values, thus raising  $D$  to 12.76, and left unsearched for a number of gradients. When finally searched,  $K_3$  increased, but by less than its initial values. The OPEP phase parameters were as for search YLAN0. A recalculation of  $D$  with all the data gave 2.28.

In connection with search YLAN2 it will be recalled that Gammel and Thaler<sup>5</sup> had calculated T=0 phase parameters at 90, 156, and 310 Mev with a phenomenological potential including a spin-orbit interaction. Gammel and Thaler, to whom the authors extend their appreciation for this assistance, made calculations available at a number of other energies from 10-140 Mev. These and the published results were used, with graphical smoothing when necessary to connect the lower and higher energy regions, in order to obtain starting values for YLAN2, with phase parameters in T=1 states still being given by YLAM(1). As in the case of YLAN0,  $\theta_5^G$  and  $\rho_5$ , though searched, were started at their OPEP values, no other convenient choice being available. The sign convention for the coupling parameter, which was reversed by Gammel and Thaler in this work compared to their previous usage, was incorrectly interpreted so that starting values of  $\rho_1$  and  $\rho_3$  had reversed signs. OPEP phase parameters were as in YLAN0. Although the original intention regarding the search was not carried out, the resultant fit is not poor and is therefore included here.

For search YLAN2M results of YLAN0, YLAN1, YLAN2 were used in  $\xi$  variations [see I, Eq. (4)]. Each of the three showed a minimum in  $D$  between the searched values, with the least minimum occurring  $\frac{3}{4}$  of the way from YLAN1 to YLAN2. Starting values for YLAN2M were obtained as  $\frac{1}{4}[3\delta_{YLAN2} + \delta_{YLAN1}]$ . Only two gradients were calculated. The OPEP phase parameters, taking into account the pion mass differences by means of Eqs. (5)-(5.3) of I and including relativistic effects,<sup>6</sup> replaced those of YLAN2.

For search YLAN3 the fit YLAM(2), referred to hereafter as "YLAM," for which the OPEP phase parameters had been calculated using the  $\pi^0$  mass and relativistically, supplied the T=1 phase parameters and

YLAN2M provided those in  $T=0$  states for  $L \leq 2$ . Since  $\delta^F_3, \theta^F_4, \rho_4$  and phase parameters in states for  $L > 3$  were given OPEP values in YLAM, consistent treatment of the  $T=0$  states indicated that  $K_3, \theta^G_3, \delta^G_4, \theta^G_5, \rho_5$  and phase parameters in states for  $L > 5$  should also be started at their OPEP values and not allowed to vary initially. The pion mass treatment of Eqs. (5)-(5.3) of I was used throughout. The five phase parameters in  $T=0$  states listed above were searched at high energies in later stages of the work.

For search YLAN3M at the end of the YLAN3 searches, the final values of  $\rho_1$  were replaced by the Gammel-Thaler starting values with account taken of their sign convention for the coupling parameter. The coupling parameter for the  $J=3$  state had moved to positive values in the YLAN3 searches, and so was not replaced. If the polarization data at 350 Mev (not included in other cases) are omitted, the final  $D$  value is 1.64.

### III. COMPARISON OF THE SEARCHES

The results of the searches are most easily compared with the aid of graphs of the phase parameters and corresponding representations of data. Figs. 1-6 show the phase parameters  $\theta^{S_1}, \rho_1, K_1, \theta^{D_1}, \delta^{D_2}, \theta^{D_3}, \theta^G_3, K_3$ ,

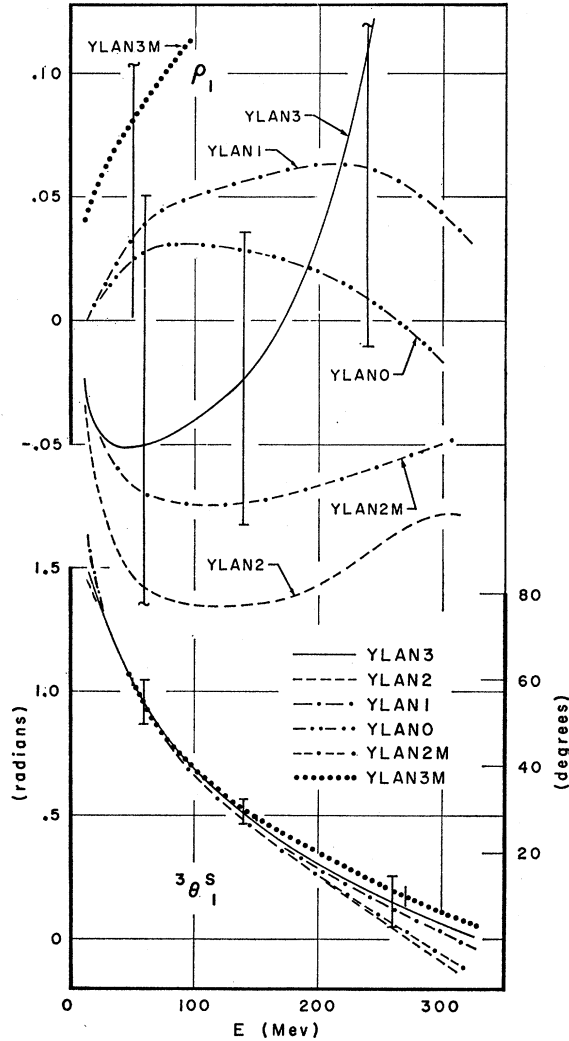


FIG. 1. Phase-parameters  $\theta^{S_1}$  for the  ${}^3S_1$  state and coupling parameter  $\rho_1$  between  ${}^3S_1$  and  ${}^3D_1$  states, plotted against energy. The value of  $\rho_1$  at 300 Mev for YLAN3M is 0.2598. In this and other figures the notation is the same as for the proton-proton analysis reported in the work cited in reference 1. In this and the following figures, curves representing the fits resulting from the searches, described in the text, are shown in a uniform convention corresponding to the key supplied: full lines for YLAN3, dotted lines for YLAN3M, dashed lines for YLAN2, etc. Error bars correspond to the "standard deviation" entries in Table V of the text. The YLAN0 values of  $\theta^{S_1}$  are so nearly equal to those for YLAN1 that the former could not be shown on the graph. The error bars on the phase-parameter graphs for case YLAN3M are drawn without serifs to distinguish them from those for case YLAN3.

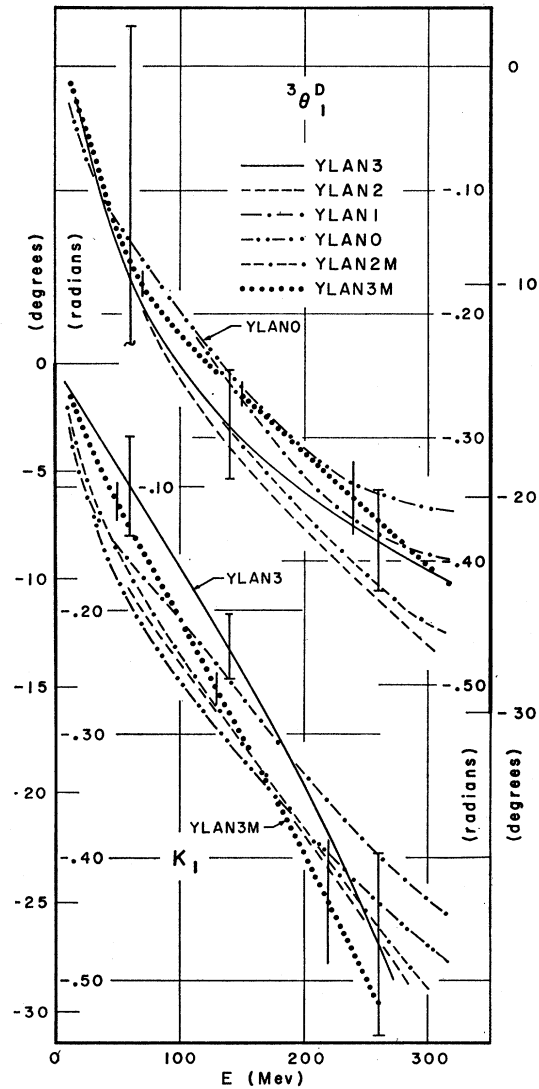


FIG. 2. Phase shift  $K_1$  in the  ${}^1P_1$  state and phase parameter  $\theta^{D_1}$  in the  ${}^3D_1$  state plotted against energy. Conventions for error bars as in Fig. 1. The error bars on the phase-parameter graphs for case YLAN3M are drawn without serifs to distinguish them from those for case YLAN3.

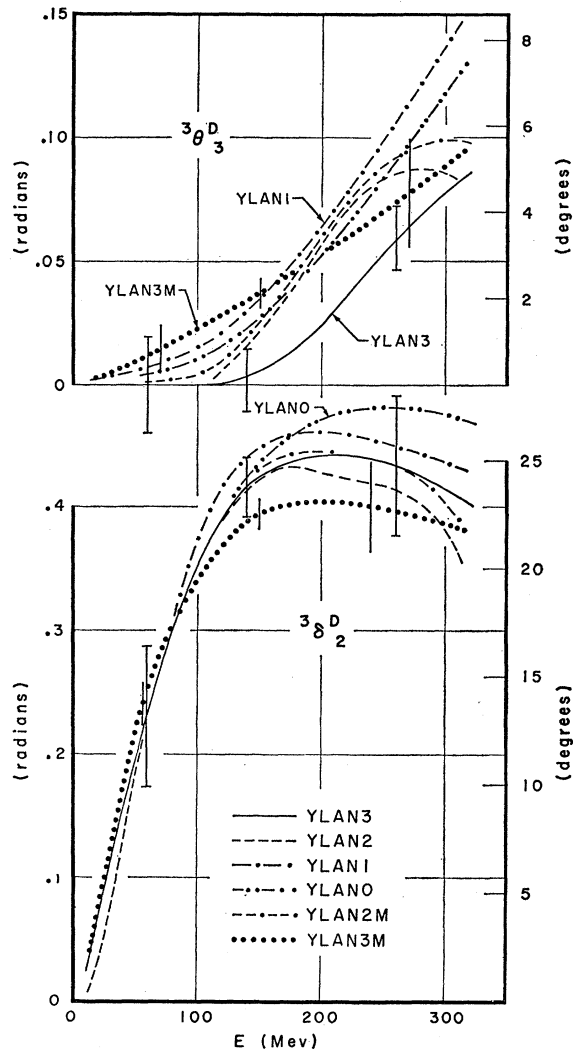


FIG. 3. Phase shift  $\delta_2^{D_2}$  in the  ${}^3D_2$  state and phase parameter  $\theta_3^{D_3}$  in the  ${}^3D_3$  state plotted against energy. Conventions for error bars as in Fig. 1. The vanishing of  $\theta_3^{D_3}$  for some fits up to relatively high energies is not meant literally. In the course of the relevant searches,  $\theta_3^{D_3}$  below 100 Mev fluctuated between small positive and negative values. No loss in quality of fit was sustained when the value was arbitrarily stabilized as zero. The error bars on the phase-parameter graphs for case YLAN3M are drawn without serifs to distinguish them from those for case YLAN3.

$\rho_3$ ,  $\delta_4^G$ ,  $\theta_5^G$ ,  $\rho_5$  as functions of energy for the searches of Table III. Figs. 7-14 give the representations provided by these phase-parameters of the data listed in Tables I and II. Figure 15 shows, for selected data, the improvement in fit produced by searches YLAN0 and YLAN3, while Fig. 16 shows the corresponding change in the phase parameters  $K_3$ ,  $\rho_3$  which accompanied the improvement in fit. Figure 17 shows representations of triple scattering data at 310 Mev provided by the searched phase parameters.

A striking feature of the search YLAN0 was the movement of  $K_3$  shown in Fig. 16. At the same time,  $K_1$  moved only by small amounts from its starting

values. Since the OPEP gives negative values for all singlet odd phase shifts, the question arose whether the data could be fitted with  $K_3$  kept negative. The YLAN1 search answered this question affirmatively. When  $K_3$ , initially restored to its starting values and fixed through several gradients, was allowed to vary, it remained negative, as shown in Fig. 4. The coupling parameter  $\rho_3$ , on the other hand, which had remained negative except at the highest energies during the YLAN0 search, attained positive values over the whole energy range in the YLAN1 search. The two fits to data are equally good, as Table III and Figs. 7-14 show, with, perhaps, a slight preference for YLAN1 indicated because of its superior fit to polarization at 95 Mev in the angular range  $50^\circ$ - $120^\circ$ , as shown in Fig. 11. The phase parameters  $K_3$  and  $\rho_3$  behaved during search YLAN2 as

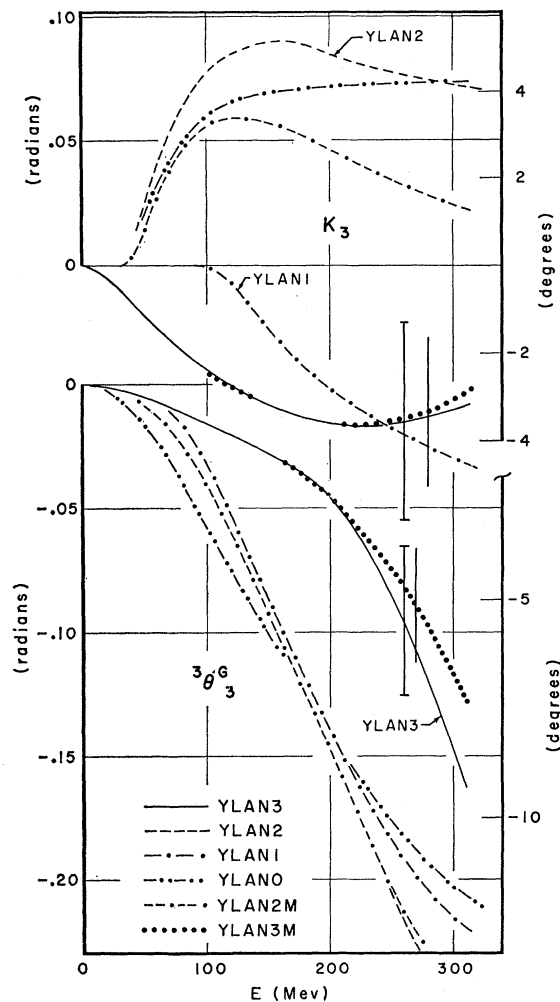


FIG. 4. Phase parameter  $\theta_3^G$  in the  ${}^3G_3$  state and phase shift  $K_3$  in  ${}^1F_3$  state plotted against energy. Conventions for error bars as in Fig. 1. For several fits,  $K_3$  is small at low energies and poorly determined by the data. It is shown as zero in these instances. The error bars on the phase-parameter graphs for case YLAN3M are drawn without serifs to distinguish them from those for case YLAN3.

they had in YLAN0, and during YLAN3 as they had in YLAN1. Figure 16 shows the results for YLAN3.

Like  $\rho_3$ , the final values of  $\rho_1$  are positive for some searches, negative for others. In all searches except YLAN3M, however,  $\rho_1$  moved in the positive direction; in YLAN3M,  $\rho_1$  was started with positive values. There is a suggestion, therefore, that  $\rho_1$  should be positive as given by the GT potential. However, as shown in Fig. 1, the statistical uncertainties in the value of  $\rho_1$  are so large that such a conclusion is rather uncertain. It is noteworthy that changes in  $\rho_1$  by amounts equal to itself can be adjusted for by small changes in other phase parameters, as comparison of searches YLAN3 and 3M shows.

In their gross features, the principal differences between the starting phase-parameter curves for YLAN0 and YLAN2, based, respectively, on the phenomono-

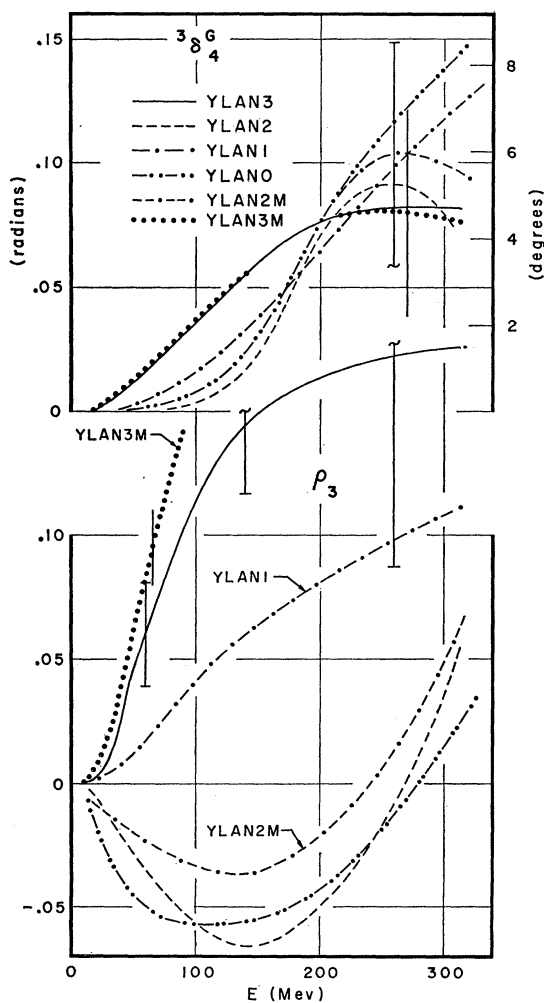


FIG. 5. The coupling parameter  $\rho_3$  between  ${}^3D_3$  and  ${}^3G_3$  states and phase shift  $\delta^G_4$  in the  ${}^3G_4$  state plotted against energy. Conventions for error bars as in Fig. 1. The value of  $\rho_3$  at 300 Mev for YLAN3M is 0.2045. The error bars on the phase-parameter graphs for case YLAN3M are drawn without serifs to distinguish them from those for case YLAN3.

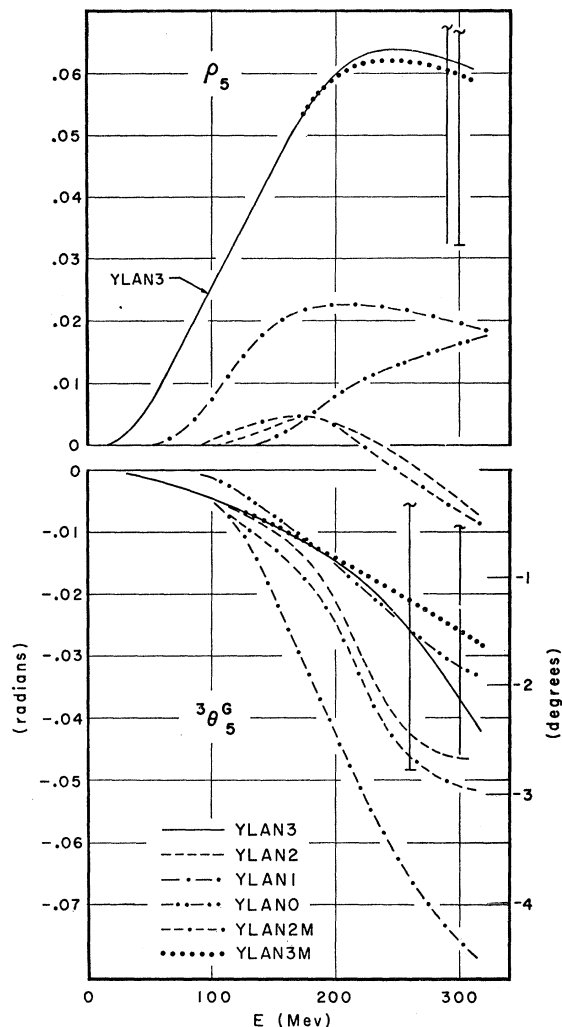


FIG. 6. Phase parameter  $\theta^G_5$  in  ${}^3G_5$  state and coupling parameter  $\rho_5$  between  ${}^3G_5$  and  ${}^3I_5$  states plotted against energy. Conventions for error bars as in Fig. 1. The error bars on the phase-parameter graphs for case YLAN3M are drawn without serifs to distinguish them from those for case YLAN3.

logical potentials of GCT and GT, occur for  $\rho_1$ ,  $\delta^D_2$  at energies  $> 140$  Mev, and to a lesser extent for  $\theta^S_1$  and for  $\theta^D_1$ ,  $\theta^D_3$  at higher energies.

The final curves show that  $\theta^S_1$  has become nearly the same for all cases. Similarly,  $\delta^D_2$  and  $\theta^D_1$  exhibit only small differences for the various searches. For YLAN3 and YLAN3M,  $\theta^D_3$ ,  $\theta^G_3$ ,  $\rho_5$  and to a slight degree  $K_1$  separate from the cluster formed by curves of these phase parameters for the other cases, but even here the sign and trend with energy is similar as seen in Figs. 2, 3, 4, and 6. It is for  $\rho_1$ ,  $K_3$ , and  $\rho_3$  that the main differences among the fits occur (cf. Figs. 1, 4, and 5).

The values of  $\rho_3$  and  $K_3$  divide the fits into two classes. For the first, containing YLAN0, YLAN2, YLAN2M,  $K_3$  is positive and  $\rho_3$  negative over most of the energy

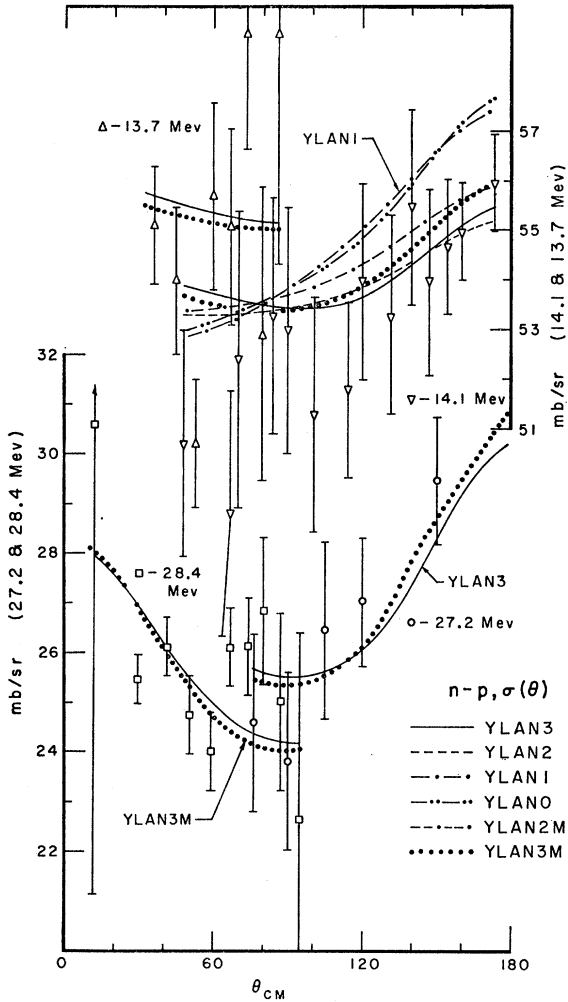


FIG. 7. Representations of the neutron-proton cross section  $\sigma(\theta)$  at 13.7, 14.1, 27.2, and 28.4 Mev as a function of center-of-mass scattering angle  $\theta$  provided by the phase parameters of Figs. 1-6, plus the phase parameters of YLAM of the proton-proton analysis in  $T=1$  states, and OPEP values for phase parameters in states of higher  $L, J$  as described in the text. The experimental results are shown for comparison, with data sources listed in Tables I and II for this and succeeding graphs. All data at the same energy are given the same symbol in this and other figures showing comparisons with data on angular distributions. Designations of the curves by dotted, dashed, full lines, etc. correspond to the phase-parameter curves of Figs. 1-6. For early searches, data at 27.2 and 28.4 Mev were run together at 27.8 Mev; they are shown separately here with YLAN3 and YLAN3M representations only, since only for these searches they were run separately. An experimental point at  $179^\circ$  for 27.2 Mev does not appear on the corresponding graph. Its value is  $(31.35 \pm 1.3)$  mb/sr, and it is fitted within the error by both YLAN3 and YLAN3M.

range, as seen in Figs. 4 and 5, while for YLAN1, YLAN3, and YLAN3M which form the second class, these phase parameters have the opposite sign.

It should be noted that with respect to  $\theta^{G_3}, \rho_3$ , and  $\theta^{G_5}$ , YLAN1 is more closely related to YLAN0, YLAN2, and YLAN2M rather than YLAN3 and YLAN3M, so that for an experimental quantity more sensitive to

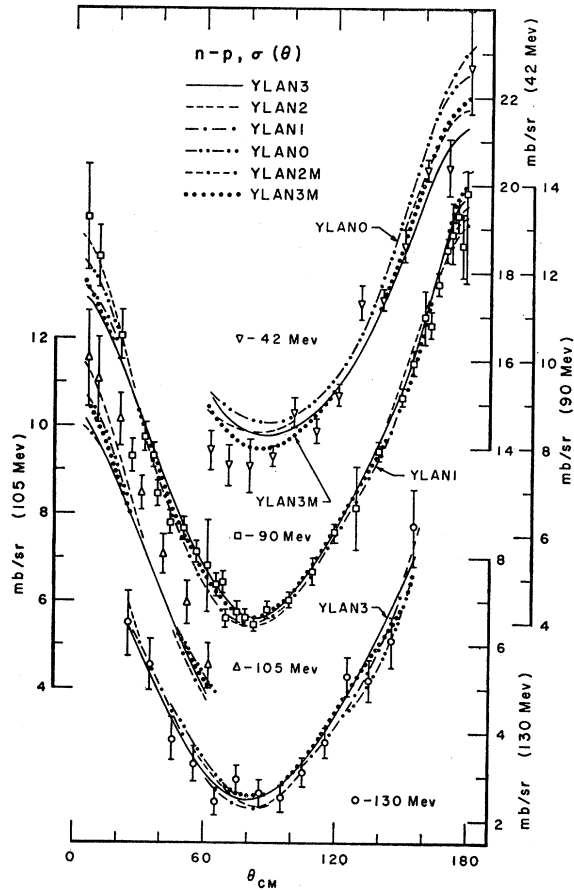


FIG. 8. Representations of the neutron-proton differential scattering cross section  $\sigma(\theta)$  at 42, 90, 105, and 130 Mev compared with experiment. The similarity of the representations for all fits is striking here. The YLAN2M fit to  $\sigma(\theta)$  at 42 Mev is omitted being essentially the same as YLAN0 at the smaller and YLAN3M at the larger angles.

these parameters than to  $K_3$  and  $\rho_3$ , YLAN1 may be expected to give representations intermediate between those of YLAN3, 3M, and of YLAN0, 2, 2M. For the data available at present, however, there is some evidence that YLAN1 is properly grouped with YLAN3, 3M. This evidence arises from an inspection of results of  $\xi$  variations, a procedure described in I, Eq. (4).

A  $\xi$  variation between YLAN1 and YLAN2 has a slight shoulder in the plot of  $D$  against  $\xi$  at about the midpoint, while between YLAN1 and YLAN0 there is a broad flat minimum in the  $D$  values. For a  $\xi$  variation between YLAN0 and YLAN2, the  $D$  values plotted against  $\xi$  form a smooth, nearly parabolic curve, as is the case between YLAN3 and YLAN3M. A definite shoulder appears, however, in the  $\xi$  variation between YLAN0 and YLAN3M. Thus there is no case where a shoulder appears in a plot of  $D$  against  $\xi$  for pairs of fits in the same  $\rho_3, K_3$  class, while for pairs in different classes a shoulder appears in two cases, and a broad, flat minimum in another. These results partially support the view that the fits studied may be considered

as forming two families of which YLAN3M and YLAN2 are representative members. The sign of  $\rho_1$  appears not to distinguish members of the same family since only minor differences in the other phase parameters are required to change the sign of  $\rho_1$ . As the fits to data and  $D$  values show, the available  $n$ - $p$  measurements do not select between the two families. In fact, the fits are not especially sensitive even to the replacement of the YLAM values for the  $T=1$  phase parameters by their YRB1 values. When this replacement was made in the YLAN3 fit, the  $D$  value only increased by about 0.1. It may be noted that according to I, YRB1 is probably in the same depression of the  $D$  value surface in phase-parameter space as YLAM and the insensitivity of YLAN3 to the difference between YLAM and YRB1 is therefore not altogether surprising. Since YLAM and YRB1 are far from being identical, the result appeared, nevertheless, to be noteworthy.

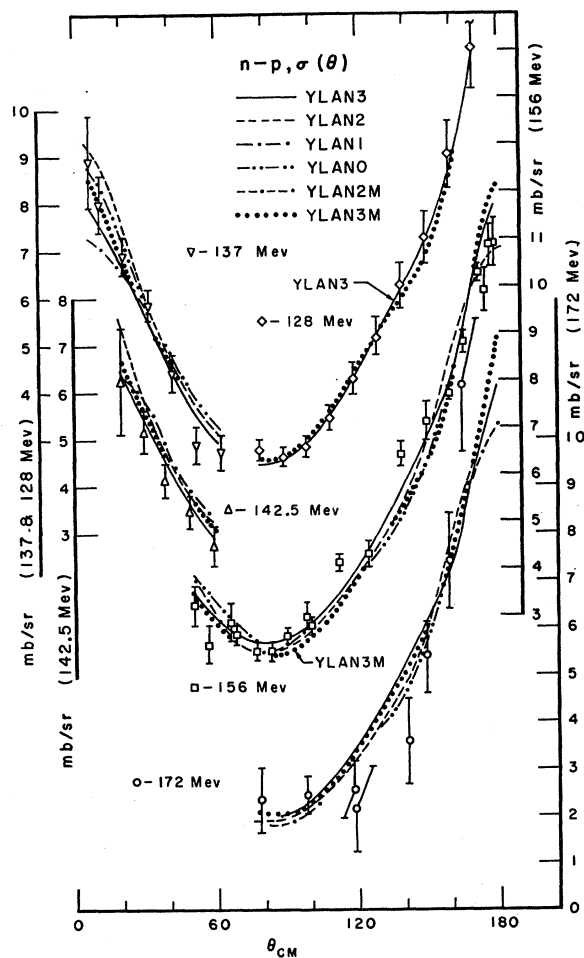


FIG. 9. Representations of the neutron-proton differential scattering cross section,  $\sigma(\theta)$ , for 128, 137, 142.5, 156, and 172 Mev compared with experiment. The 128-Mev data were available only for the later stages of the YLAN3 search and for YLAN3M. An experimental point at  $180^\circ$  for 172 Mev could not be conveniently shown. Its value is  $17.1 \pm 7.0$  mb/sr. Both YLAN3 and 3M fits are inside its error bars.

After completion of the searches, the new cross-section data of Scanlon, Stafford, Thresher, and Bowen<sup>7</sup> became available in a preliminary form. These data give 137 ratios of  $\sigma(\theta)$  to  $\sigma(173^\circ)$  at 14 energies from 27.5 to 120 Mev. Comparison of these ratios with values calculated from YLAN1, YLAN2, and YLAN3M gave equally good representations of the data by all three fits and on the basis of other experience similar results may be expected of the other fits. The experimental uncertainties on the data are too large to allow a selection of one of the fits over another, as is the case for other cross-section data.

Work of Bowen, Cox, Huxtable, Langford, Scanlon

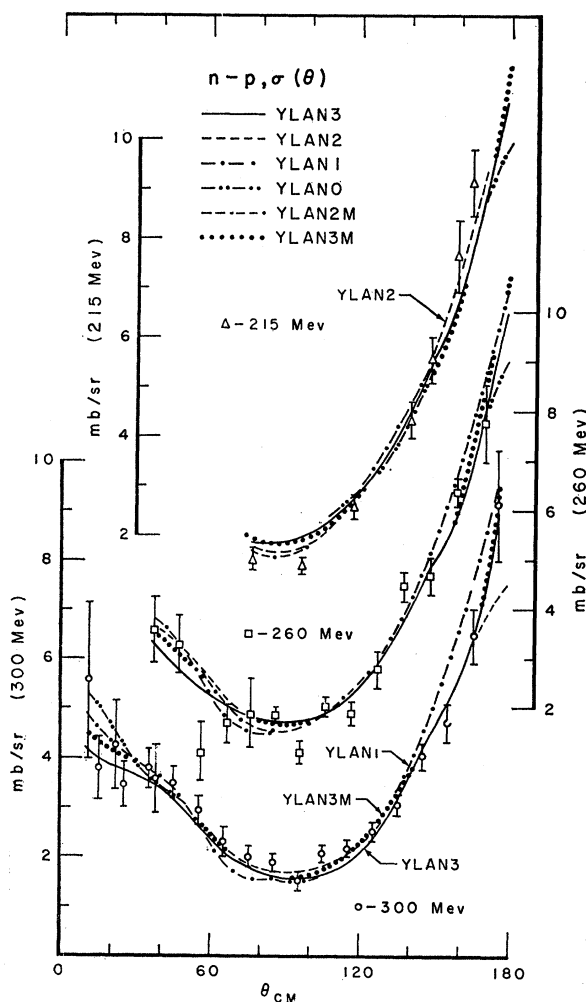


FIG. 10. Representations of the neutron-proton differential scattering cross section at 215, 260, and 300 Mev compared with experiment. Experimental points at  $180^\circ$  for 215 and 260 Mev, having values of  $13.8 \pm 2.9$  and  $13.7 \pm 2.1$  mb/sr, respectively, could not be conveniently shown. The YLAN3 and 3M fits are just outside the error bars in both cases.

<sup>7</sup> J. P. Scanlon, G. H. Stafford, J. J. Thresher, and P. H. Bowen (private communication). The authors wish to thank Dr. Stafford for making these results available in advance of publication.

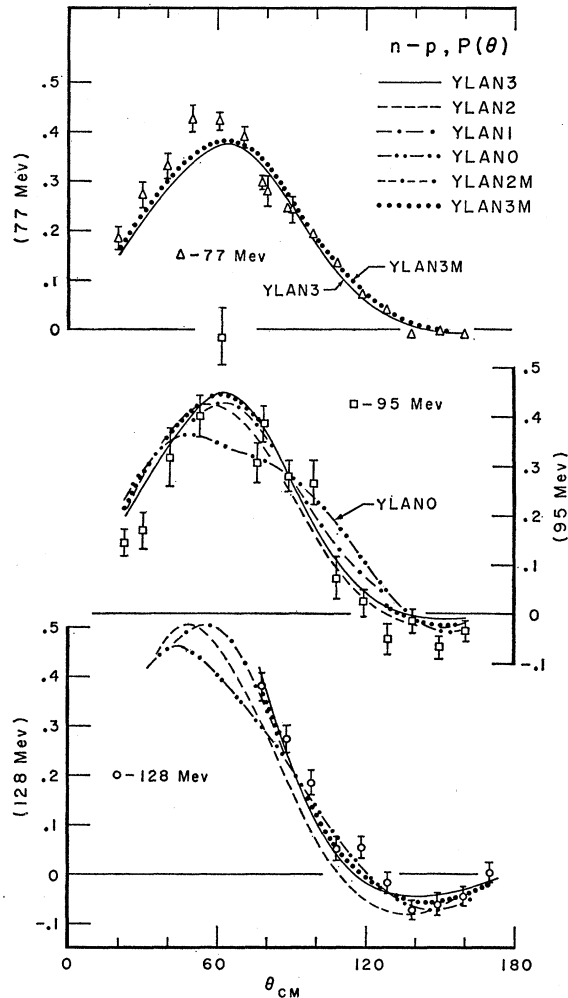


FIG. 11. Representations of the neutron-proton polarization  $P(\theta)$  at 77, 95, and 128 Mev compared with experiment. The data at 77 Mev were available only after the completion of all searches except YLAN3 and 3M.

and Thresher<sup>8</sup> on  $n$ - $p$  polarization has also been compared with the representations supplied by the fits. In this case YLAN0, YLAN1, YLAN3M were used to calculate  $P(\theta)$  at  $20^\circ$ ,  $30^\circ$ ,  $40^\circ$ ,  $50^\circ$ ,  $60^\circ$ ,  $80^\circ$  for energies in the range 20 to 90 Mev. The theoretical curves are all good representations of the data, and as with other polarization data shown in Figs. 11, 12, and 14 no fit is selected in preference to others by the measurements.

The phase parameters of YLAN3 and YLAN3M have been adjusted by the parallel shift method in three energy regions. As described in I following Eq. (4.1), this adjustment allows each phase parameter to change by energy-independent increments so as to improve the fit to data in a restricted energy range and tests the stability of the fit obtained with data at all

<sup>8</sup> P. H. Bowen, G. C. Cox, G. Huxtable, A. Langsford, J. P. Scanlon, and J. J. Thresher, (private communication). The authors are indebted to Dr. Basil Rose for supplying them with graphs of these data.

energies to possible variations in a limited energy interval. The adjustment was calculated for  $T=1$  and  $T=0$  phase parameters varied separately, and results are contained in Tables IV and V. All data available in the indicated energy ranges and referred to in Tables I and II were used. At the same time, standard deviations in the phase parameters, computed by the method discussed in I and given by Eq. (2.5) of that paper, were obtained and are listed in Tables IV and V following the  $\pm$  sign.

A comparison of Table IV with Table IV of I for the  $p$ - $p$  analysis shows that the  $T=1$  phase parameters are not as well determined in the present case. There is no instance of the standard deviations in Table IV of the present paper being smaller than corresponding ones for the  $p$ - $p$  analysis. They may in fact be as much as an order of magnitude larger. Since there are twice as many phase parameters included in the present analysis, the sensitivity of the quality of data representation

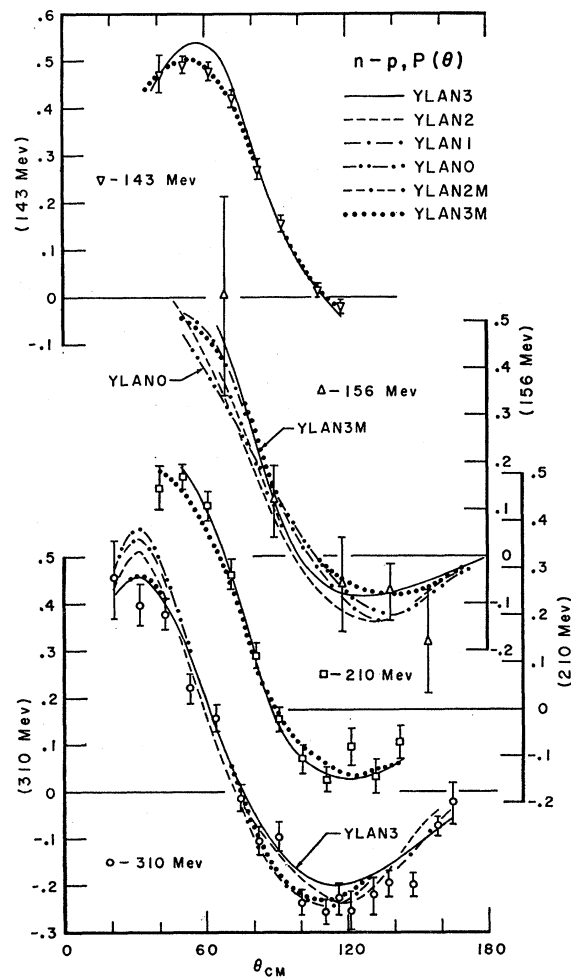


FIG. 12. Representations of the neutron-proton polarization  $P(\theta)$  at 143, 156, 210, and 310 Mev compared with experiment. The data at 143 and 210 Mev were available only for the final stages of the YLAN3 search and for YLAN3M.

to changes in the  $T=1$  phase parameters may be expected to be smaller. Also, the  $n$ - $p$  data frequently have larger uncertainties than the  $p$ - $p$  data and there are fewer types of data. All three conditions contribute to the increase in standard deviations as compared with the  $p$ - $p$  case. Intercomparing the two fits listed in Table IV, one sees that the standard deviations are consistently smaller, though probably not significantly so, for YLAN3M.

The results of parallel shift adjustment, which shows shifts usually much smaller than the standard deviation and only a few barely larger, attests to the stability of the fit to different energy emphasis. Since these  $T=1$  phase parameters also provide a fit to the  $p$ - $p$  data, consistency with the charge independence hypothesis is demonstrated lending further support to the conclusions of Breit, Hull, Lassila, and Pyatt.<sup>9</sup>

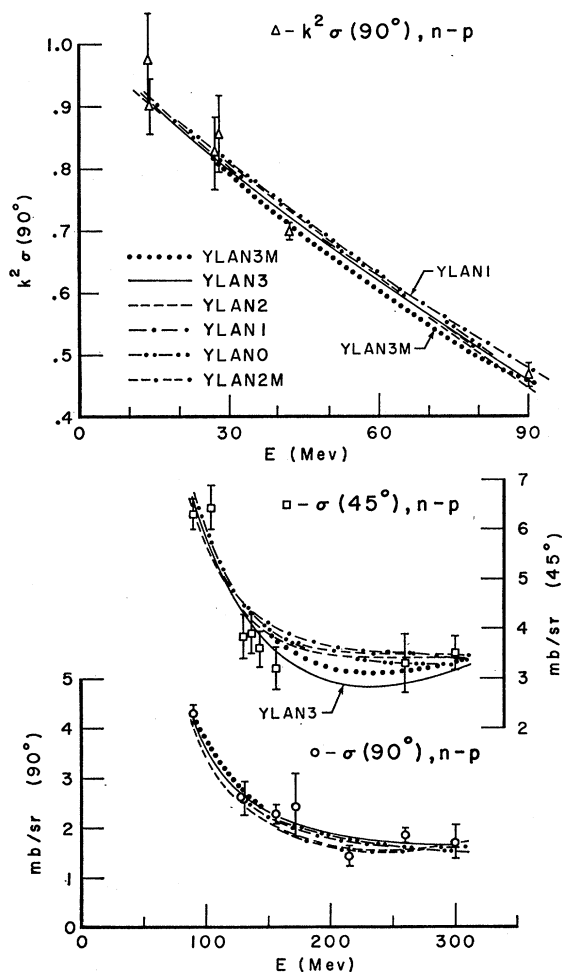


FIG. 13. Representations of  $k^2\sigma(\theta)$  and  $\sigma(\theta)$  at  $90^\circ$  and  $\sigma(\theta)$  at  $45^\circ$  as functions of energy compared with experiment. Too little data were available to permit a plot of  $k^2\sigma(45^\circ)$  for the low energies.

<sup>9</sup> G. Breit, M. H. Hull, K. E. Lassila, and K. D. Pyatt, Phys. Rev. Letters 4, 79 (1960).

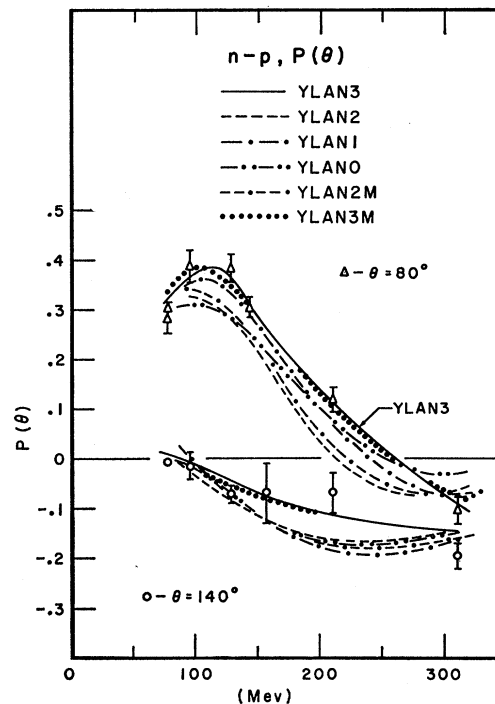


FIG. 14. Representations of  $P(\theta)$  for  $\theta=80^\circ$  and  $140^\circ$  as a function of energy compared with experiment. Lack of data prevented comparisons at other angles.

In Table V, similar information is recorded for the  $T=0$  phase parameters. Here, the standard deviations for YLAN3M are notably smaller than those for YLAN3, especially in the lower energy range. Over all, the  $T=0$  parameters are as well determined as those in  $T=1$  states by the  $n$ - $p$  data, and the stability of the fit to changes in emphasis on various energy ranges is maintained.

#### IV. TRIPLE SCATTERING

The data available in  $n$ - $p$  triple scattering are confined to preliminary unpublished results of Fischer<sup>10</sup> at 310 Mev. In these experiments, the neutron target was in the form of deuterium and polarized protons were used as projectiles. The scattered protons were analyzed and for many of the angle settings the recoil neutron was counted in coincidence. The quantities measured were Wolfenstein's  $R$  and  $D$  triple scattering parameters.<sup>11</sup> For the  $R$  measurements, the neutron recoil was monitored only at two proton scattering angles; the  $n$ - $p$  values of  $R$  at other angles were obtained by subtraction from deuteron values on the assumption that the target nucleons were free. These data were not used in the analysis, but are compared with predictions of the various fits in Fig. 17. All cases give equally good fits to the  $D$  measurements. In the

<sup>10</sup> D. L. Fischer, University of California Radiation Laboratory Report UCRL-3281, 1956 (unpublished).

<sup>11</sup> L. Wolfenstein, Phys. Rev. 96, 1654 (1954).

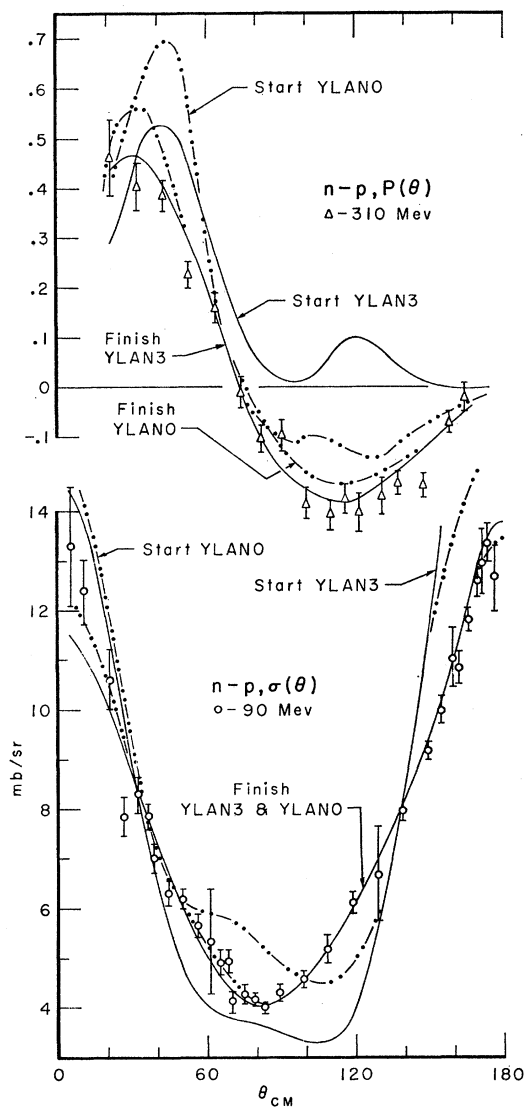


FIG. 15. Illustrations of improvements in fits produced through searches YLAN3 and YLAN0. Comparisons are for  $\sigma(\theta)$  at 90 Mev and  $P(\theta)$  at 310 Mev.

case of  $R$ , while the general magnitude of theoretical and experimental results is in agreement, the trends with angle are not similar. The theoretical curves cannot be significantly changed toward the experimental trend without affecting adversely the fits to cross section and polarization in the same energy range. Additional measurements of  $R$  at 310 Mev and other energies would therefore be of interest.

The observables discussed here are not well suited for distinguishing between the fits obtained, as Fig. 17 shows. Other calculations show, however, that at 210 Mev,  $R$  for YLAN3 and 3M separates from predicted values for YLAN0, 1, 2, 2M especially between  $70^\circ$  and  $100^\circ$  cm, that  $A(\theta)$  could distinguish YLAN3 and 3M from the other fits at low (150 Mev) and high (310

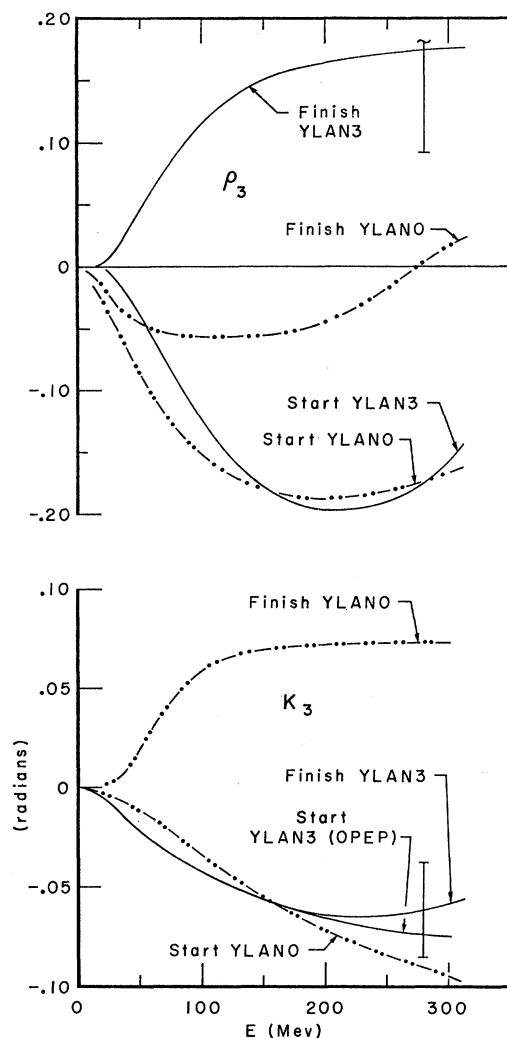


FIG. 16. Examples of changes produced in the phase parameters by the searches which gave the improvement in fit shown in Fig. 15. The parameters shown are  $K_3$  and  $\rho_3$ . For the latter the YLAN3 start is the negative of the Gammel-Thaler value.

Mev) energies in the same angular range, and that  $D(\theta)$  remains relatively insensitive. If measurements of  $R$  or  $D$  of the type where the incident particle is a polarized neutron and the scattered proton is analyzed can be carried out or if the correlation coefficient  $C_{nn}(\theta)$  can be measured, then not only might the two classes suggested above be distinguished, but YLAN1 could be separated. On the other hand, YLAN1 is not markedly different from YLAN0, 2, 2M in the measurements where both the incident and analyzed particles are protons. Values of triple scattering parameters  $D$ ,  $R$ , and  $A$  for polarized incident protons and analyzed emergent neutrons and of the correlation coefficient  $C_{nn}$  are more sensitive to the differences between YLAN1 and YLAN0, 2 and 2M regarding values of some of the phase parameters and between YLAN1 and YLAN3 and 3M regarding the values of others than measure-

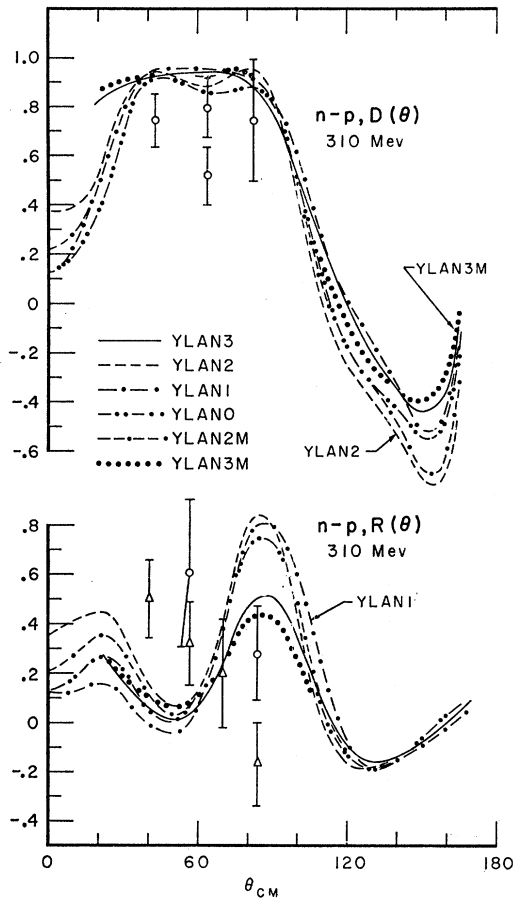


FIG. 17. Representations of the triple scattering depolarization parameter,  $D(\theta)$ , and rotation of polarization,  $R(\theta)$ , plotted against center of mass angle  $\theta$  compared with preliminary unpublished data of Fischer. In the  $R(\theta)$  plot, the points given as circles were obtained with the recoil neutron from the deuteron target monitored, while points shown as triangles were obtained by subtraction from the measured proton-deuteron rotation.

ments of  $D$ ,  $R$ , and  $A$  for polarized incident protons and analyzed emergent protons. There are even restricted angular ranges (low and high angles) where the predictions of YLAN3 and 3M for this type  $R$  and  $D$  may differ enough to be distinguished experimentally from each other. At about 50 Mev,  $C_{nn}$  measurements may be able also to distinguish YLAN3 from 3M.

## V. DISCUSSION

The final values of  $\theta^{S_1}$  for all cases cluster about the GCT values over most of the energy range and about the GT values at the lower energies. The differences between the various fits are usually smaller than the difference between GCT and GT except at the lowest energy. At 13.7 Mev, the value of  $\theta^{S_1}$  ranges from 1.638 rad for YLAN1 to 1.465 rad for YLAN2, as may be seen in Fig. 1. The uncertainties in the data in this energy region, indicated in Fig. 7, allow the wide variation in  $\theta^{S_1}$ . It is assumed that the effective-range treat-

ment is valid for the lower energies not included in these searches, and within the indicated uncertainty in  $\theta^{S_1}$  it is possible to join present results smoothly to those of the effective-range approximation. The values of  $\rho_1$  for YLAN3M have decreased from the GT start by about 0.05 at 100 Mev, 0.02 at 200 Mev and by a smaller amount at 300 Mev. From Table V it is seen that the decrease is just outside the calculated uncertainty for this parameter at 100 Mev, but within it at the higher energies. The YLAN3 values of  $\rho_1$  are quite different from the starting value;  $-0.05$  compared to the starting value of  $-0.13$  at 60 Mev, and positive for  $E > 165$  Mev while the start continues negative for the whole energy range. YLAN2 has the least values, reading  $-0.11$  at 100 Mev, but is still larger than its starting value of  $-0.16$  at this energy. The insensitivity of the fits to data to precise values of  $\rho_1$  has already been mentioned. It appears that slight adjustments of other parameters can allow for any value of  $\rho_1$  between 0.15 and  $-0.10$ .

The GCT curve for  $\theta^{D_1}$  turns up at high energies corresponding to an increase in the value of this parameter with energy in the region from 220 to 300 Mev. This feature of the GCT curve has disappeared in the final fits. YLAN0 gives  $-0.33$  at 300 Mev for  $\theta^{D_1}$  in comparison with  $-0.29$  in the case of GCT and values well below that of YLAN0 have resulted from other fits; YLAN2 gave  $-0.47$  at this energy. YLAN3 and 3M straddle the GT start: YLAN3M is 0.008 radian higher at 150 Mev, where YLAN3 is 0.01 lower, and at about 300 Mev the values of  $\theta^{D_1}$  are nearly equal for GT, YLAN3, and YLAN3M. The YLAN3 and 3M uncertainties cover the starting values.

For  $K_1$ , YLAN3 and 3M graphs of phase parameters are concave when viewed from the energy axis, while the others are convex. The sign of the curvature is like that of the GT start at the higher but not at the lower energies, while the graphs for the remaining fits have the same sign of curvature as the graph for GCT. Thus at 100 Mev YLAN3 is 0.04 rad larger than GT, and YLAN3M is 0.09 rad larger, while at 250 Mev, YLAN3M is nearly equal to GT, and YLAN3 is 0.05 rad larger than GCT at 100 Mev, and bracket GCT at 300 Mev.

The graphs of  $\delta^{D_2}$  show a maximum at energies below 300 Mev for all of the fits and are in this respect like GT but unlike GCT. YLAN3M is lower than GT, however, by 0.07 rad at 200 Mev and 0.02 rad at 300 Mev. YLAN3 is 0.03 rad lower at 200 Mev and nearly equal to GT at 300 Mev. YLAN1, though started as GCT, is nearly 0.3 rad lower at 300 Mev, and nearly reproduces GT.

In the case of  ${}^3\theta^{D_3}$ , the negative values at low energies for the GCT start have disappeared, and the large value of 0.25 rad at 300 Mev has become only 0.15 rad for YLAN0. The rapid rise with energy of  ${}^3\theta^{D_3}$  for both GCT and GT is not reflected in any fit except YLAN2,

TABLE IV. Standard deviations and displacements of YLAM phase parameters calculated with  $n$ - $p$  data for YLAN3 and YLAN3M. The entry is given by the number and the power of 10 by which it should be multiplied.

Energy range and search		Standard deviations and shifts of phase parameters in T=1 states.						
		Values in radians except for $\rho_2^a$						
		$K_0$	$\delta^{P_0}$	$\delta^{P_1}$	$\theta^{P_2}$	$\rho_2$	$\theta^{P_2}$	$K_2$
13.7-95 Mev	YLAN3	$\pm 5.0(-2)$	$\pm 1.5(-1)$	$\pm 5.7(-2)$	$\pm 4.5(-2)$	$\pm 5.8(-2)$	$\pm 2.8(-2)$	$\pm 1.8(-2)$
	YLAN3M	$-4.6(-3)$	$-3.3(-3)$	$+4.6(-3)$	$-1.2(-2)$	$+2.1(-3)$	$+6.8(-3)$	$-1.7(-3)$
105-172 Mev	YLAN3	$\pm 5.5(-1)$	$\pm 5.0(-1)$	$\pm 7.6(-2)$	$\pm 2.3(-2)$	$\pm 4.7(-2)$	$\pm 5.2(-2)$	$\pm 9.2(-2)$
	YLAN3M	$-9.1(-4)$	$+1.9(-3)$	$+2.4(-3)$	$+1.2(-2)$	$-4.0(-3)$	$+7.6(-3)$	$-8.8(-3)$
215-310 Mev	YLAN3	$\pm 2.0(-1)$	$\pm 3.2(-1)$	$\pm 5.8(-2)$	$\pm 6.9(-2)$	$\pm 1.0(-1)$	$\pm 5.7(-2)$	$\pm 3.3(-2)$
	YLAN3M	$+4.2(-4)$	$+1.1(-3)$	$+1.7(-2)$	$-2.0(-2)$	$+2.0(-2)$	$-2.9(-2)$	$+1.5(-2)$
		$\pm 1.7(-1)$	$\pm 1.6(-1)$	$\pm 3.3(-2)$	$\pm 2.3(-2)$	$\pm 8.8(-2)$	$\pm 3.6(-2)$	$\pm 2.3(-2)$
		$+7.1(-4)$	$+5.8(-3)$	$+5.8(-3)$	$-1.4(-2)$	$+5.0(-3)$	$-1.1(-2)$	$+6.4(-3)$

<sup>a</sup> In the highest energy range,  $\delta^{P_3}$ ,  $\theta^{P_4}$ , and  $\rho_4$  were included in the error determination and parallel shift gradient. The standard deviations of these quantities in that range are  $\pm 7.4(-2)$ ,  $\pm 4.7(-2)$ ,  $\pm 3.8(-2)$ , respectively, for YLAN3, and  $\pm 7.2(-2)$ ,  $\pm 2.3(-2)$ ,  $\pm 2.9(-2)$ , for YLAN3M. Their shifts are  $+3.9(-3)$ ,  $+1.2(-2)$ ,  $-5.1(-3)$ , respectively, for YLAN3, and  $-5.7(-3)$ ,  $+6.2(-3)$ ,  $-4.6(-3)$ , for YLAN3M.

which practically vanishes at an unreasonably high energy of  $\sim 100$  Mev and appears improbable so far as the representation of this parameter is concerned. YLAN3M varies more gently with energy, crosses the GT start at 70 Mev, is 0.14 rad smaller at 200 Mev and about 0.10 rad smaller at 300 Mev. YLAN3 practically vanishes below 100 Mev, and has the smallest values of  $\theta^{P_3}$  of any fit at all energies: It is 0.20 rad smaller than GT at 200 Mev, and 0.12 rad smaller at 300 Mev. The vanishing of the fitted values of  ${}^3\theta^{P_3}$  at unexpectedly large energies has no literal significance, the uncertainties in the determination of the phase parameters being large as seen in Table V.

The behavior of  $K_3$  and  $\rho_3$  has already received some attention. Both GCT and GT as well as OPEP values are negative for  $K_3$  and YLAN1, 3, and 3M remain negative. YLAN3 deviates only slightly from its OPEP start at high energies, and its calculated uncertainty includes the starting value. The same is true of YLAN3M. For  $\rho_3$ , the fitted values are all positive for

YLAN1, 3, 3M and predominantly negative for YLAN0, 2, 2M. There is little resemblance to starting values: YLAN0, 2, 2M are all larger by 0.10 or more than GCT or the negative of GT, while YLAN1, 3 are not even of the same sign. YLAN3M started as GT, and GT is found to be 0.03 low at 100 Mev, and about 0.10 low at 300 Mev. The last compared point illustrates the fact that the relatively sharp maximum of the GT plot of  $\rho_3$  against energy is not found in any of the final fits.

For  ${}^3\theta^{G_3}$ , the fitted values for YLAN0, 1, 2, 2M are much smaller than those for GCT: These fits cluster about a value of about  $-0.14$  rad at 200 Mev compared to  $-0.08$  rad for GCT, and about  $-0.23$  rad at 300 Mev compared to  $-0.105$ . YLAN3 and 3M were started at the OPEP values of  ${}^3\theta^{D_3}$ , and have moved from it toward those for GCT, but are left between the GCT and GT values. They are within each other's uncertainty, nearly four standard deviations lower than OPEP at 300 Mev. For  ${}^3\delta^{G_4}$ , GT and GCT bracket the

TABLE V. Standard deviations and displacements of T=0 phase parameters for YLAN3 and YLAN3M. The entry is given by the number and the power of 10 by which it should be multiplied.

Energy range and search		Standard deviations and shifts of phase parameters in T=0 states.						
		Values in radians except for $\rho_1, \rho_3^a$						
		$\theta^{S_1}$	$\rho_1$	$\theta^{D_1}$	$K_1$	$\delta^{D_2}$	$\theta^{D_3}$	$\rho_3$
13.7-95 Mev	YLAN3	$\pm 8.8(-2)$	$\pm 1.0(-1)$	$\pm 2.1(-1)$	$\pm 4.0(-1)$	$\pm 5.7(-2)$	$\pm 3.9(-2)$	$\pm 2.1(-2)$
	YLAN3M	$-8.6(-3)$	$+6.2(-4)$	$+9.8(-4)$	$-3.7(-3)$	$-4.1(-3)$	$-1.7(-3)$	$-7.5(-4)$
105-172 Mev	YLAN3	$\pm 1.6(-2)$	$\pm 8.0(-2)$	$\pm 1.5(-2)$	$\pm 1.1(-2)$	$\pm 1.8(-2)$	$\pm 1.0(-2)$	$\pm 1.5(-2)$
	YLAN3M	$-4.4(-3)$	$-1.6(-3)$	$-9.2(-3)$	$-6.0(-3)$	$-3.3(-3)$	$-1.6(-3)$	$+1.3(-3)$
215-310 Mev	YLAN3	$\pm 5.3(-2)$	$\pm 5.9(-2)$	$\pm 4.4(-2)$	$\pm 2.8(-2)$	$\pm 2.4(-2)$	$\pm 2.2(-2)$	$\pm 2.7(-2)$
	YLAN3M	$+7.1(-3)$	$-2.4(-3)$	$-5.3(-4)$	$+9.7(-3)$	$+1.5(-2)$	$+2.9(-3)$	$+7.5(-3)$
215-310 Mev	YLAN3	$\pm 9.8(-3)$	$\pm 3.5(-2)$	$\pm 1.3(-2)$	$\pm 9.0(-3)$	$\pm 1.2(-2)$	$\pm 6.0(-3)$	$\pm 1.2(-3)$
	YLAN3M	$-3.8(-4)$	$-3.9(-3)$	$+3.7(-3)$	$+4.9(-3)$	$+2.1(-3)$	$-6.0(-3)$	$+1.3(-3)$
215-310 Mev	YLAN3	$\pm 9.9(-2)$	$\pm 1.4(-1)$	$\pm 4.1(-2)$	$\pm 7.4(-2)$	$\pm 5.6(-2)$	$\pm 2.7(-2)$	$\pm 8.5(-2)$
	YLAN3M	$+8.2(-4)$	$-2.2(-3)$	$+3.2(-3)$	$-5.2(-3)$	$-7.7(-3)$	$+1.0(-2)$	$-3.6(-3)$
		$\pm 3.9(-2)$	$\pm 9.9(-2)$	$\pm 5.0(-2)$	$\pm 3.0(-2)$	$\pm 3.7(-2)$	$\pm 2.2(-2)$	$\pm 5.9(-2)$
		$+3.3(-3)$	$+7.5(-4)$	$-9.8(-4)$	$+4.6(-3)$	$-1.9(-3)$	$+6.8(-3)$	$-1.0(-2)$

<sup>a</sup> In the highest energy range,  $K_3$ ,  $\theta^{G_3}$ ,  $\delta^{G_4}$ ,  $\theta^{G_5}$ , and  $\rho_5$  were also searched. The standard deviations of these quantities were, respectively,  $\pm 4.1(-2)$ ,  $\pm 3.0(-2)$ ,  $\pm 6.7(-2)$ ,  $\pm 2.8(-2)$ ,  $\pm 3.0(-2)$  for YLAN3, and  $\pm 3.0(-2)$ ,  $\pm 2.3(-2)$ ,  $\pm 4.2(-3)$ ,  $\pm 2.0(-2)$ ,  $\pm 2.8(-2)$ , for YLAN3M. The shifts of the quantities are, respectively,  $-7.6(-3)$ ,  $-3.7(-3)$ ,  $+1.5(-2)$ ,  $-8.4(-3)$ ,  $+1.6(-3)$  for YLAN3, and  $-4.4(-3)$ ,  $+9.0(-3)$ ,  $-5.8(-3)$ ,  $+1.2(-3)$  for YLAN3M.

OPEP values, and YLAN3, 3M reflect this situation in the fits. They are lower than OPEP by 0.04 rad at 300 Mev, but as Table V shows, the difference is within the relatively large uncertainty for this phase parameter. The other fits are smaller than either GCT or GT values at low energies, but YLAN0 and 1 approach the GCT values at 300 Mev, while for YLAN2 and 2M the plots of phase shift against energy go through a maximum and then approach GT.

Both  $\theta_5^G$  and  $\rho_5$  were started at OPEP values for all cases, and YLAN3, 3M differ from the start only at high energies. YLAN3 is 0.014 rad lower than OPEP at 300 Mev for  $\theta_5^G$ , but this is within the statistical uncertainty; YLAN3M is nearly the same as OPEP. YLAN0, 2, 2M are all within the uncertainty limit on the YLAN3 value of  $\theta_5^G$ , but YLAN1 is more negative than OPEP by 0.03 rad at 200 Mev and 0.054 rad at 300 Mev. In the case of  $\rho_5$ , the YLAN0, 1, 2, 2M fitted values are much smaller than OPEP values, and YLAN2, 2M are negative above 250 Mev. YLAN3, 3M have values rather close together, deviate only at large energies from OPEP where they are about 0.036 smaller at 300 Mev, a difference of about 1.5 standard deviations.

The most striking difference between the phase parameters of the YLAN3, 3M fits is in the case of  $\rho_1$ , as has already been suggested. However, even in this case the uncertainty limits of the two fits overlap, and the differences in their predictions for the measured quantities are expected to be minor. The data points and theoretical curves of Figs. 7-14 and Fig. 17 confirm this supposition. The insensitivity of the cross-section data to the values of  $\rho_1$  is strikingly illustrated in Fig. 8: at 90 Mev the fits all group close together, while Fig. 1 shows the greatest separation in the values of  $\rho_1$  in this energy region. There appears to be no significant effect on the polarization and triple scattering predictions either. It is true, of course, that other phase parameters have adjusted themselves for changes in  $\rho_1$ , but that such adjustments are small has already been brought out. This is in contrast to the influence of  $\rho_3$ , which is about the same size as  $\rho_1$ . Major readjustments, at least in  $K_3$ , are required to maintain fits to data when  $\rho_3$  changes sign. There seems, however, to be an insensitivity to changes in sign of  $\rho_3$  and  $K_3$ , provided that their signs are opposite to each other. Thus YLAN1 predicts different results for measurements than do YLAN0, 2, 2M only for some triple scattering parameters as yet unobserved.

The question of the sign of  $K_3, \rho_3$  has some bearing on the determination of the distance at which the OPEP becomes effective,<sup>6</sup> since the fitted values of these phase parameters have the same sign as predicted by the OPEP for YLAN1, 3, 3M and opposite for YLAN0, 2, 2M. The values of  $K_3$  in searches YLAN3, 3M are close to the OPEP values, as may be seen by comparing Fig 4 and Fig. 16; their uncertainties easily include the potential values. For  $\rho_3$  the searched values in cases YLAN3, 3M are smaller at high energies than OPEP differing from it by  $\sim 2$  standard deviations at 300 Mev. However, in a first order estimate, modifications in OPEP needed to reproduce YLAN3, 3M appear to be small compared to those needed for YLAN0, 2, 2M.

As in the case of the  $p$ - $p$  analysis reported in I, potentials applicable to states of sharp  $J$  and parity have been sought which can represent the phase parameters as a function of  $E$ . Conditions on the logarithmic derivative of the wave function, discussed in I, Sec. V would then be automatically satisfied.

The search was conducted by assuming potentials of the form suggested by Bryan's work on the  $p$ - $p$  case,<sup>12</sup>

$$V(x) = (\sum a_n x^{-n}) e^{-2x} + \text{OPEP},$$

with the  $a_n$  treated as adjustable parameters. Gradient searches in the space of the  $a_n$  were conducted individually for each  $J$  and parity, and potentials have been found to give a satisfactory fit to the YLAN3M phase parameters, although some details of the YLAN3M curves are not exactly reproduced at the present stage of the potential adjustment. The resulting potentials have a general resemblance to others published in the literature. Work is continuing on the problem of fitting the phase parameters with central, tensor, and spin-orbit potentials adjusted simultaneously in all states.

#### ACKNOWLEDGMENTS

The participation in the early stages of the work by Dr. K. D. Pyatt, Jr., is gratefully acknowledged and the expert mathematical assistance of Miss J. Gibson is much appreciated. The cooperation of the staff of the AEC Computing and Applied Mathematics Center at New York University in scheduling machine time and advice in machine operation have been of great value.

<sup>12</sup> R. A. Bryan, Bull. Am. Phys. Soc. 5, 35 (1960), and preprint kindly supplied by Dr. Bryan.